

Section 3.3

Statistical Properties: The Tycho Catalogue

3.3. Statistical Properties: The Tycho Catalogue

In this section some statistical properties of the data in the Tycho Catalogue are presented. As in the previous section, for a number of parameters distributions over the entire sky, and frequency histograms are given.

Many features of the data shown here are similar to those from the Hipparcos Catalogue; for a general description, the reader is referred to Section 3.2. Here, in general, only differences will be emphasized. Such differences result mainly from two causes: (i) the Hipparcos measurements were based on the selection of stars in the Hipparcos Input Catalogue, and therefore cannot be considered a survey; its overall statistical properties are strictly properties of the selection, and not those of a random, or complete, sample of stars. On the other hand, the entries in the Tycho Catalogue come much closer to a survey down to a certain apparent magnitude, although the limiting magnitude depends somewhat on the location on the sky (cf. Volume 4, Chapter 16); (ii) the difference in measurement geometry: while Hipparcos performed one-dimensional abscissa measurements in the direction along the scanning great circle, Tycho added information about the perpendicular direction, albeit with lower weight.

Certain of the results shown in this section are also given in Chapter 16 of Volume 4, and discussed in more detail there.

3.3.1. Density of Observed Stars and Number of Observations

The density of observed stars in the Tycho Catalogue is shown in Figure 3.3.1. Comparison with the corresponding figure for the Hipparcos Catalogue illustrates strikingly the difference in character of the two catalogues. For example, the emphasis on the Orion region present in the Hipparcos Catalogue is not present in the Tycho Catalogue. On the other hand, the difference in star density between the galactic equator and pole regions, and the low star densities in some regions (e.g. the Ophiuchus area), are emphasized in the Tycho Catalogue.

Figure 3.3.3 gives the distribution of the median number number of astrometric observations per star. This figure is very similar to that for the Hipparcos Catalogue. The features related to the sun-pointing periods visible in the Hipparcos case are absent here, since the measurements made during those periods were not used in the construction of the Tycho Catalogue. Figure 3.3.4 shows the frequency distribution of this number.

3.3.2. Standard Errors and Correlations

Sky distributions of the standard errors of the five astrometric parameters are given in Figures 3.3.5, 3.3.9, 3.3.13, 3.3.17, and 3.3.21. Frequency distributions of these standard errors are shown in Figures 3.3.6, 3.3.10, 3.3.14, 3.3.18, and 3.3.22. The

dependence of the standard errors on ecliptic latitude and on the V_T magnitude is shown in Figures 3.3.7, 3.3.11, 3.3.15, 3.3.19, and 3.3.23, and in Figures 3.3.8, 3.3.12, 3.3.16, 3.3.20, and 3.3.24, respectively. It is interesting to note the differences between the ecliptic latitude dependence shown here and the corresponding dependencies for the Hipparcos Catalogue. The overall shape of the curves is similar, but details differ: for example, the marked minimum near $\beta \sim \pm 47^\circ$ is present for all five parameters, whereas in the Hipparcos case it was only visible for the longitudinal ones. This illustrates the difference in measurement geometry between the two cases. Also, the curve for σ_π is much smoother for the Tycho than for the Hipparcos case, probably for the same reason.

The astrometric correlations are distributed over the sky as shown in Figures 3.3.25 to 3.3.34. For a general discussion on these correlations, see Section 3.2.3. Frequency histograms for the correlations are combined in Figure 3.3.35.

Differences with respect to the Hipparcos Catalogue are present in the histograms. There is a marked asymmetry in the correlations between α^* and μ_{α^*} , and δ and μ_δ . These asymmetries indicate that the mean effective epoch of the Tycho Catalogue is somewhat later than that of the Hipparcos Catalogue, in accordance with Equations 1.2.6 and 1.2.8, due to a different weighting of the two types of observation towards the end of the mission. On the other hand, the asymmetry in the correlation between declination and parallax present in the Hipparcos Catalogue is much smaller in the case of the Tycho Catalogue, due to the measurement geometry of Tycho. There is an additional magnitude-related effect: for stars fainter than $V_T = 10$ mag, there is no asymmetry; for brighter stars, there is an effect, but always smaller than in the case of the Hipparcos Catalogue measurements.

Figures 3.3.36 and 3.3.37 give the results for the goodness-of-fit indicator F2. The distribution over the sky turns out to be much less uniform than that shown for the Hipparcos Catalogue. Note that F2 was not considered a reliable parameter for use in the construction of the Tycho Catalogue, and the values should be used with great care (see Section 16.2 of Volume 4).

3.3.3. Photometric Data

Results for the B_T and V_T magnitudes and their standard errors are shown in Figures 3.3.38 to 3.3.43. The sky distributions of the median B_T and V_T magnitudes show a strong relationship with the scanning pattern, but the heavily scanned regions at $\beta \sim \pm 47^\circ$ are not particularly visible here.

The sky distribution of the median (Johnson) colour index $B - V$ is presented in Figure 3.3.44. Differences with the corresponding figure for the Hipparcos Catalogue again show clearly the marked difference in character of the two catalogues. The present figure represents the statistical properties of the galactic solar neighbourhood to 100–250 pc. North of the galactic centre the dust complexes in Ophiuchus and Scorpius cause red and reddened stars to dominate. In the galactic plane, intrinsically brighter stars are over-represented, as expected for a magnitude-limited catalogue, leading to extra early-type stars. This is particularly true in the region $180^\circ < l < 270^\circ$ where there is less interstellar absorption. The emphasis of the Hipparcos Catalogue on the Orion region and the galactic meridians $l = 0^\circ$ and $l = 180^\circ$ is absent, as expected.

The frequency histogram, Figure 3.3.45, of the $B - V$ colour index shows two maxima, the one near $B - V = 0.5$ mag corresponding to the high concentration of stars near the turn-off point in the Hertzsprung-Russell diagram, and the other near $B - V = 1$ mag being due to the G8-K0 giants in the core helium-burning phase. The two other peaks present in the corresponding figure for the Hipparcos Catalogue were due to selection effects of that catalogue, and are therefore much less prominent here.

Figure 3.3.46 shows the distribution of the standard error of the $B - V$ colour index. Figure 3.3.47 gives the distribution for the scatter s in the V_T magnitudes.



Figure 3.3.1. Tycho Catalogue: number of observed stars per square degree, in galactic coordinates (cell size $2^\circ \times 2^\circ$).

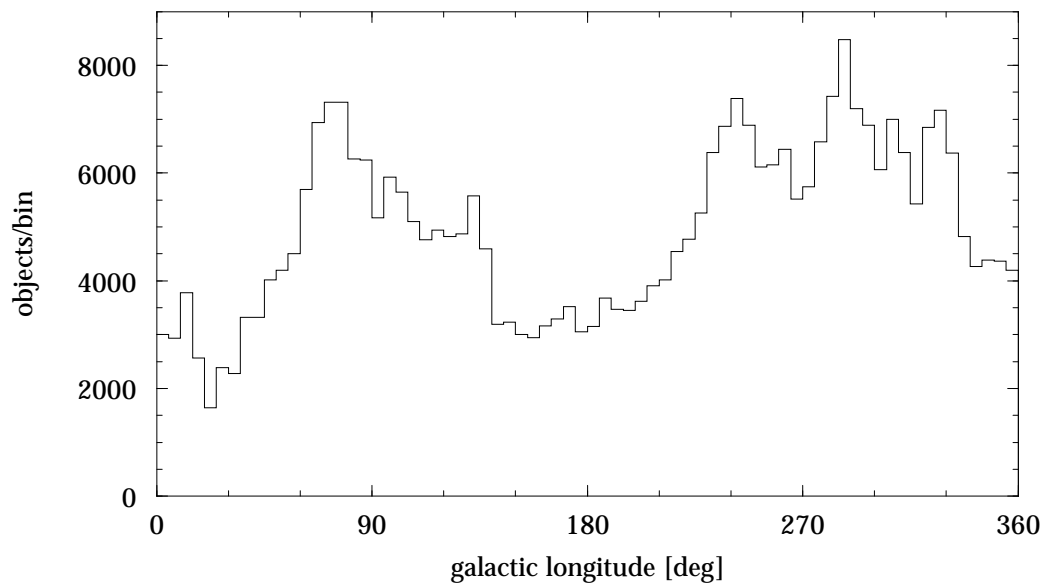


Figure 3.3.2. Tycho Catalogue: distribution of number of stars near the galactic equator ($b < 10^\circ$, bin size 5°).



Figure 3.3.3. Tycho Catalogue: mean number of observations per star, in ecliptic coordinates (cell size $3^\circ \times 3^\circ$).

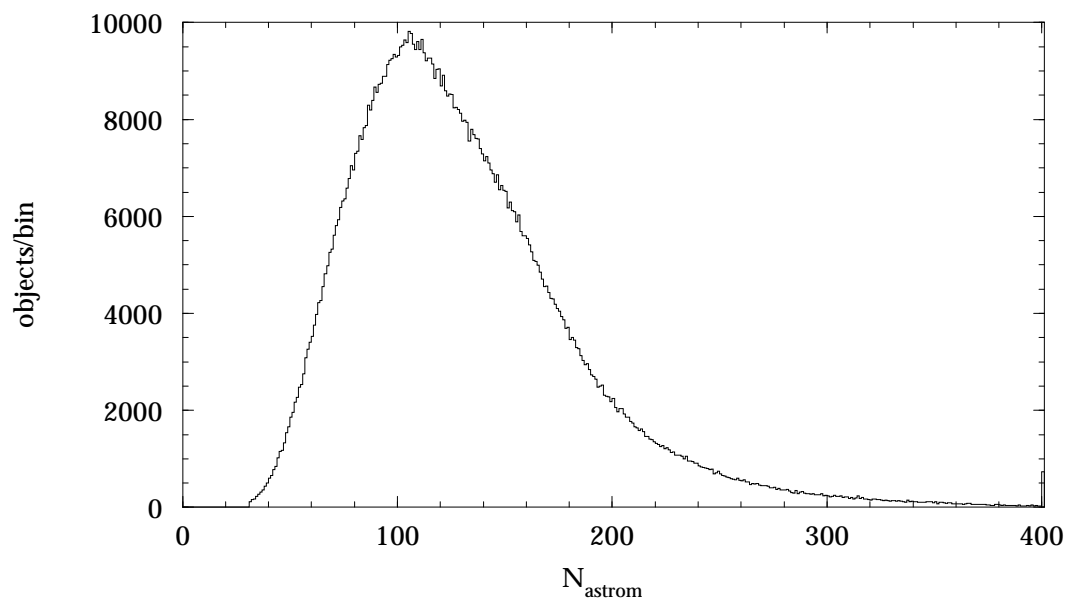


Figure 3.3.4. Tycho Catalogue, Field T29: number of transits retained in the astrometric adjustment (bin size 1). The rightmost bin contains all values above 400.



Figure 3.3.5. Tycho Catalogue, Field T14: median standard error of α^* , in ecliptic coordinates (cell size $3^\circ \times 3^\circ$).

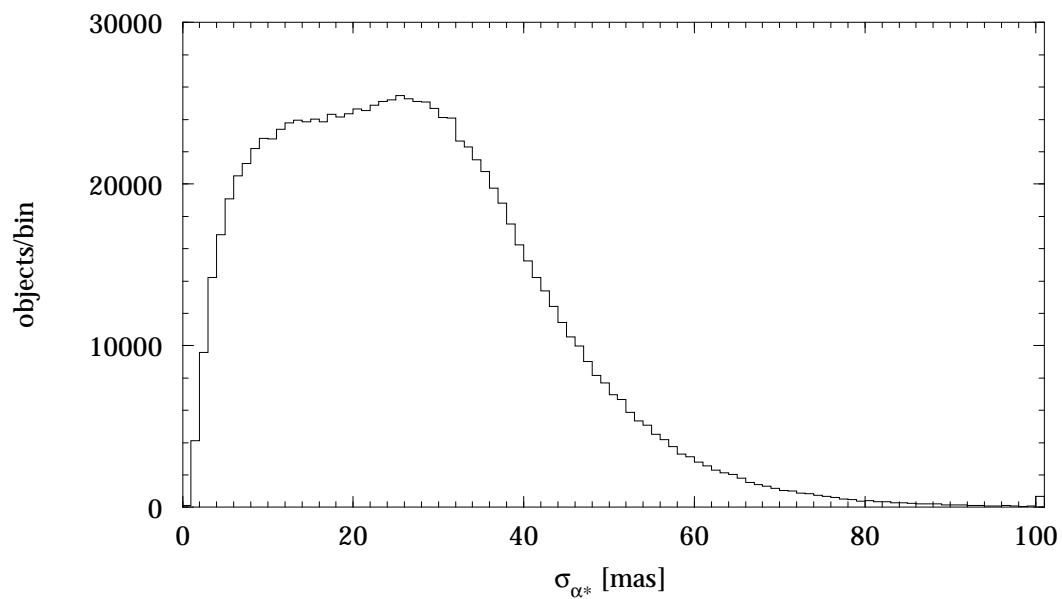


Figure 3.3.6. Tycho Catalogue, Field T14: standard error of α^* (bin size 1 mas). The rightmost bin contains all values above 100 mas.

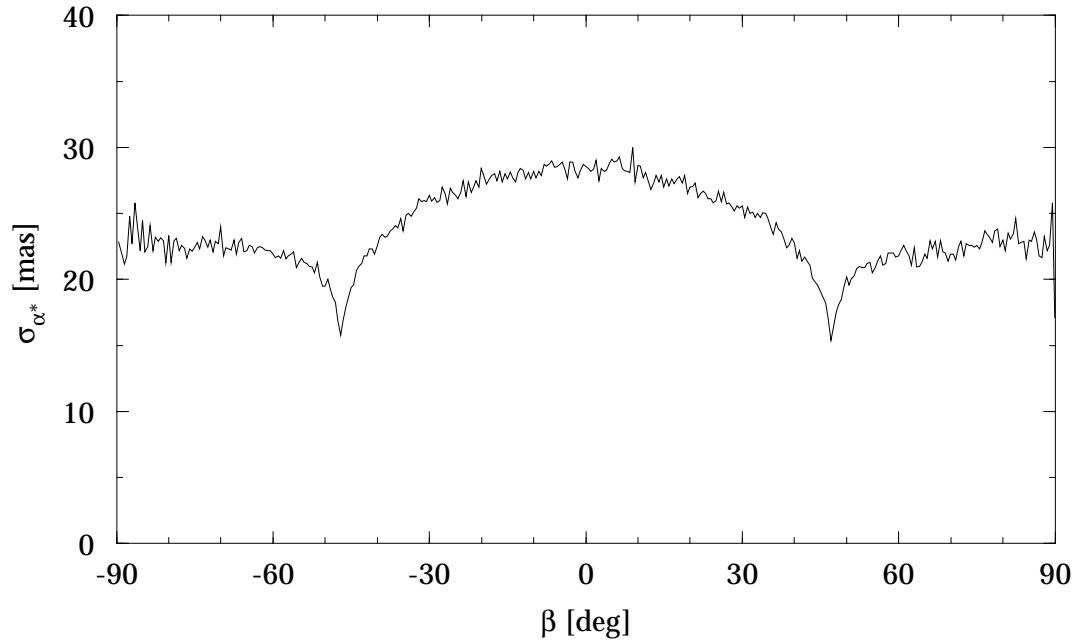


Figure 3.3.7. Tycho Catalogue, Field T14: median standard error of α^* versus ecliptic latitude (bin size 0.5°).

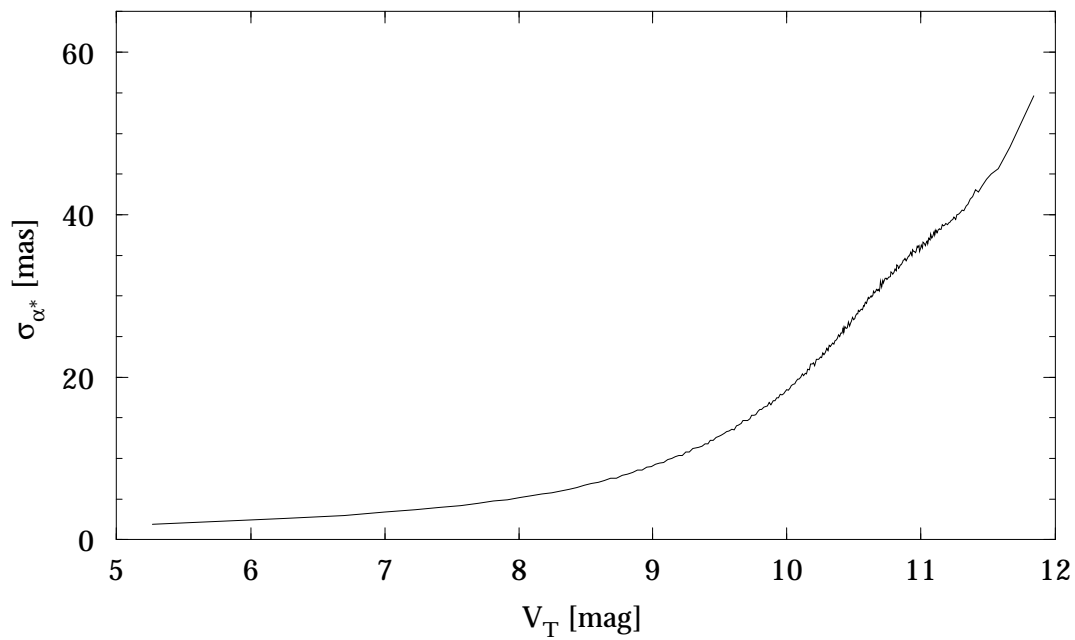


Figure 3.3.8. Tycho Catalogue, Field T14: median standard error of α^* versus V_T (bin size 0.05 mag).



Figure 3.3.9. Tycho Catalogue, Field T15: median standard error of δ , in ecliptic coordinates (cell size $3^\circ \times 3^\circ$).

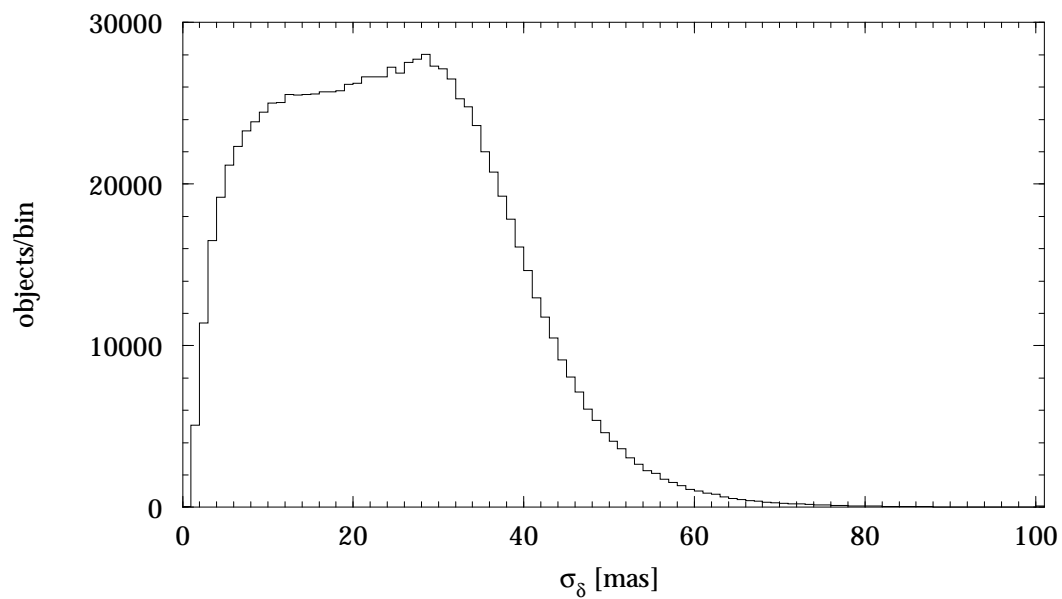


Figure 3.3.10. Tycho Catalogue, Field T15: standard error of δ (bin size 1 mas). The rightmost bin contains all values above 100 mas.

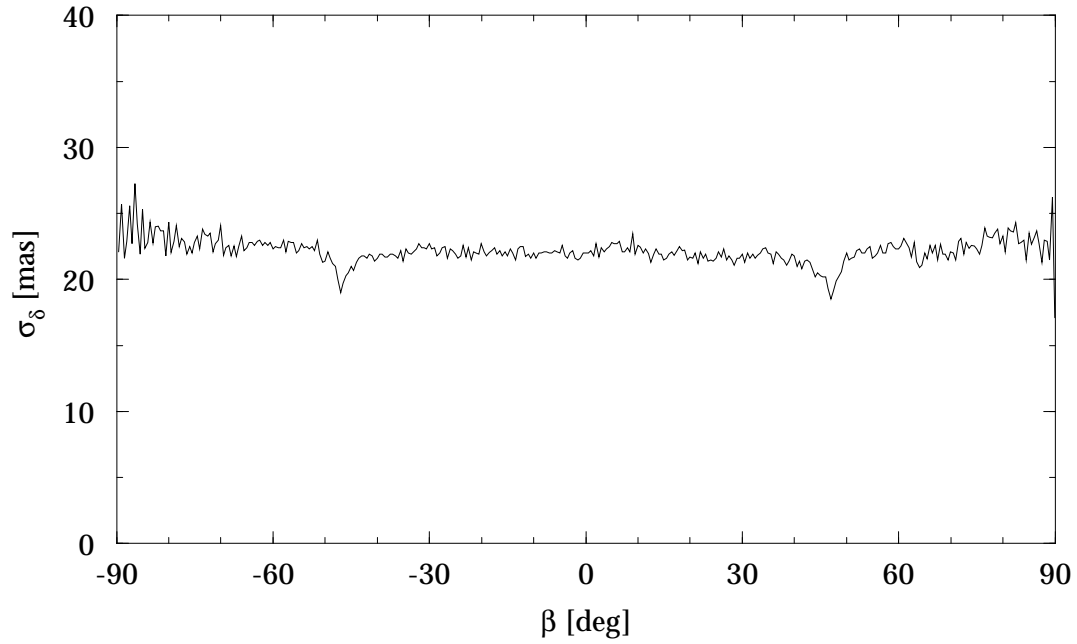


Figure 3.3.11. Tycho Catalogue, Field T15: median standard error of δ versus ecliptic latitude (bin size 0.5°).

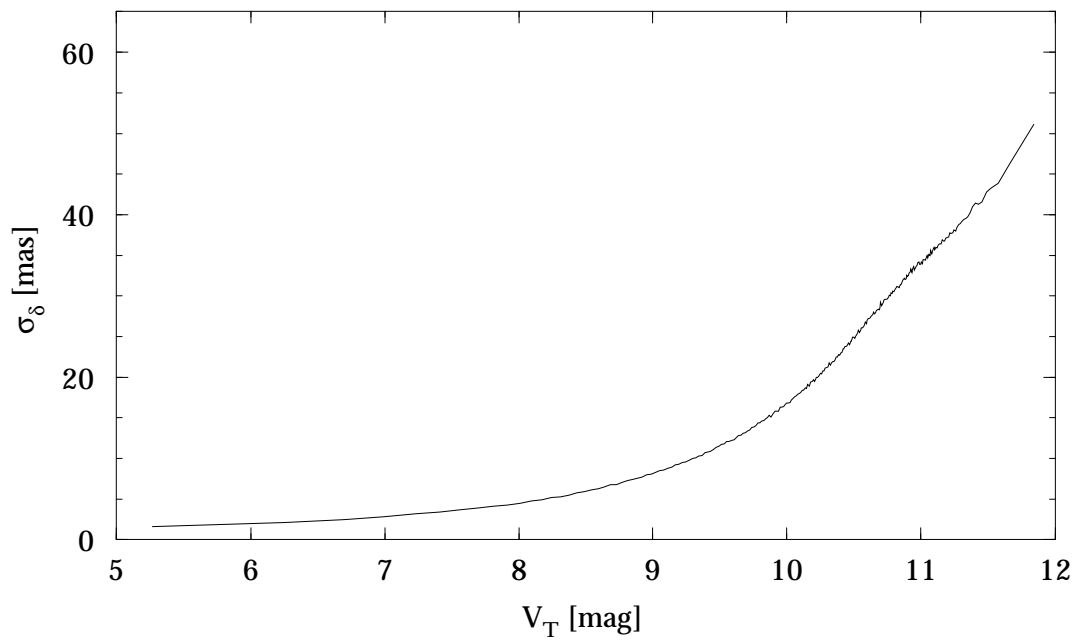


Figure 3.3.12. Tycho Catalogue, Field T15: median standard error of δ versus V_T (bin size 0.05 mag).



Figure 3.3.13. Tycho Catalogue, Field T16: median standard error of π , in ecliptic coordinates (cell size $3^\circ \times 3^\circ$).

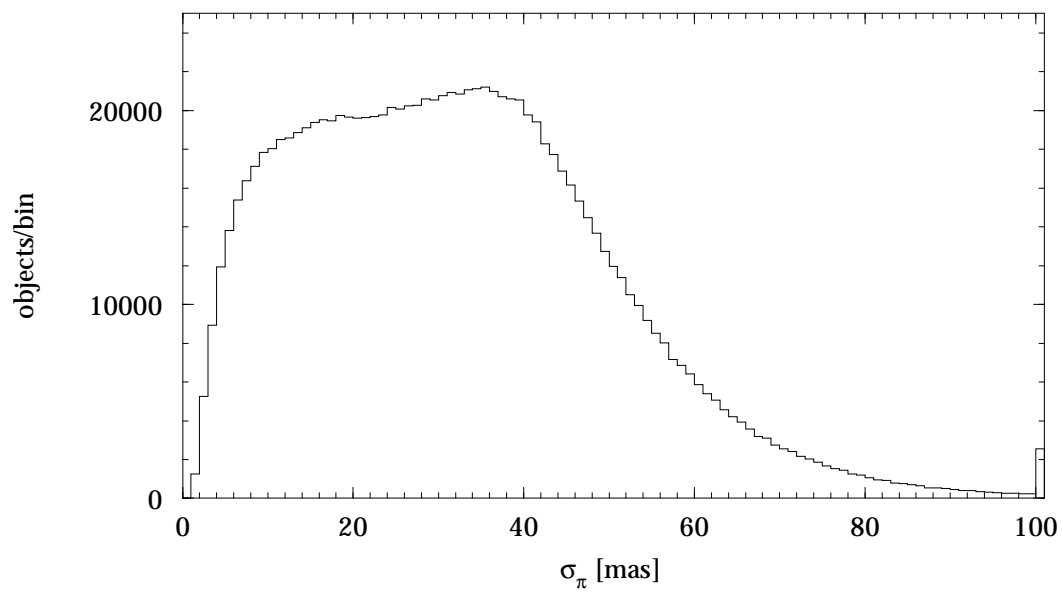


Figure 3.3.14. Tycho Catalogue, Field T16: standard error of π (bin size 1 mas). The rightmost bin contains all values above 100 mas.

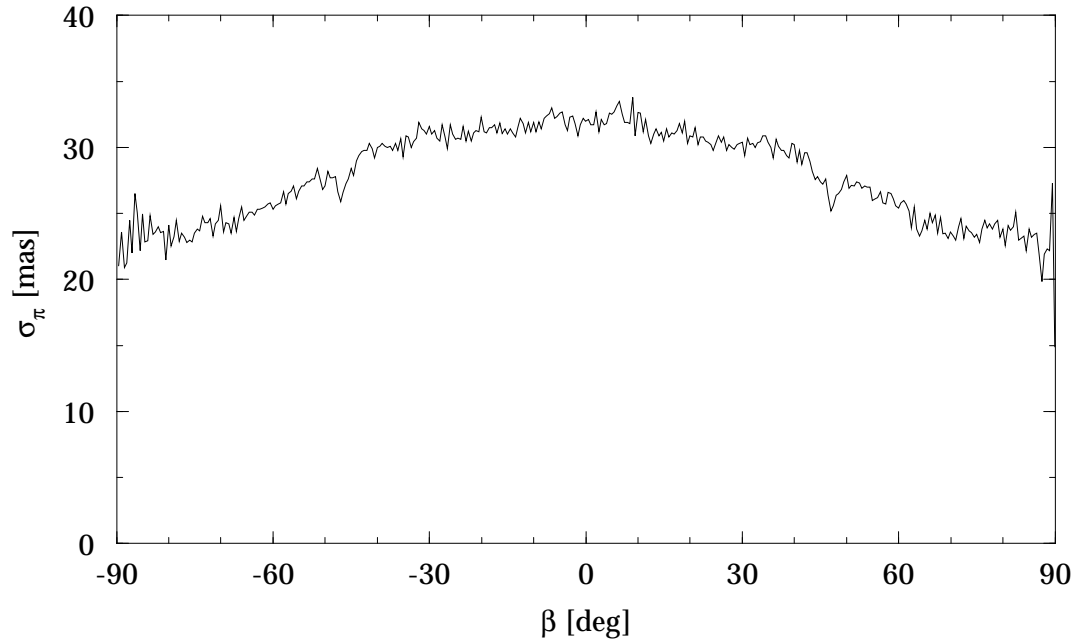


Figure 3.3.15. Tycho Catalogue, Field T16: median standard error of π versus ecliptic latitude (bin size 0.5°).

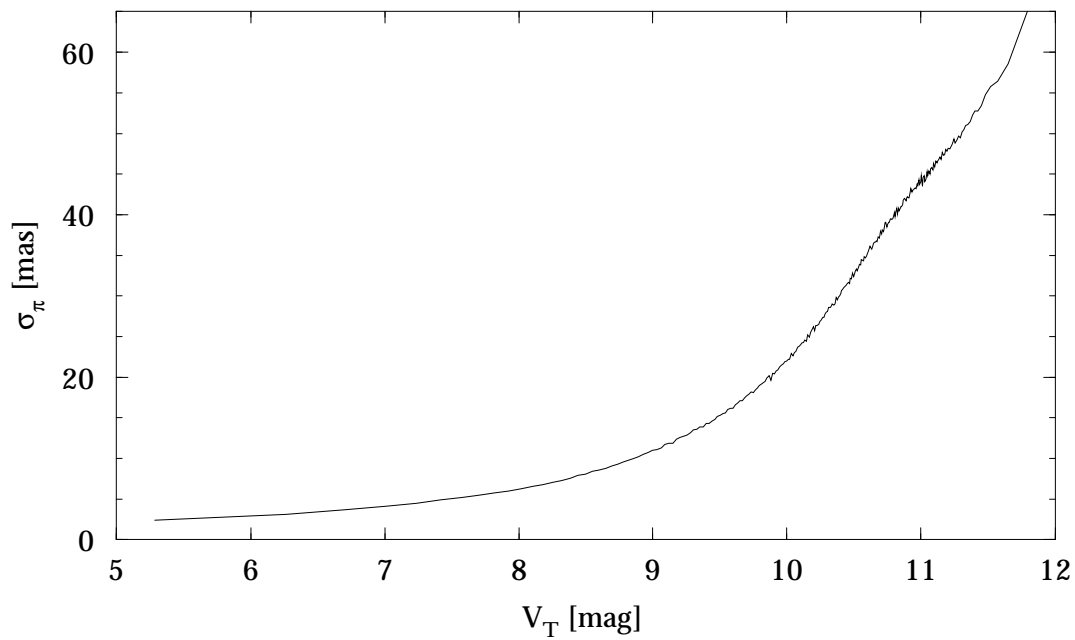


Figure 3.3.16. Tycho Catalogue, Field T16: median standard error of π versus V_T (bin size 0.05 mag).



Figure 3.3.17. Tycho Catalogue, Field T17: median standard error of μ_{α^*} , in ecliptic coordinates (cell size $3^\circ \times 3^\circ$).

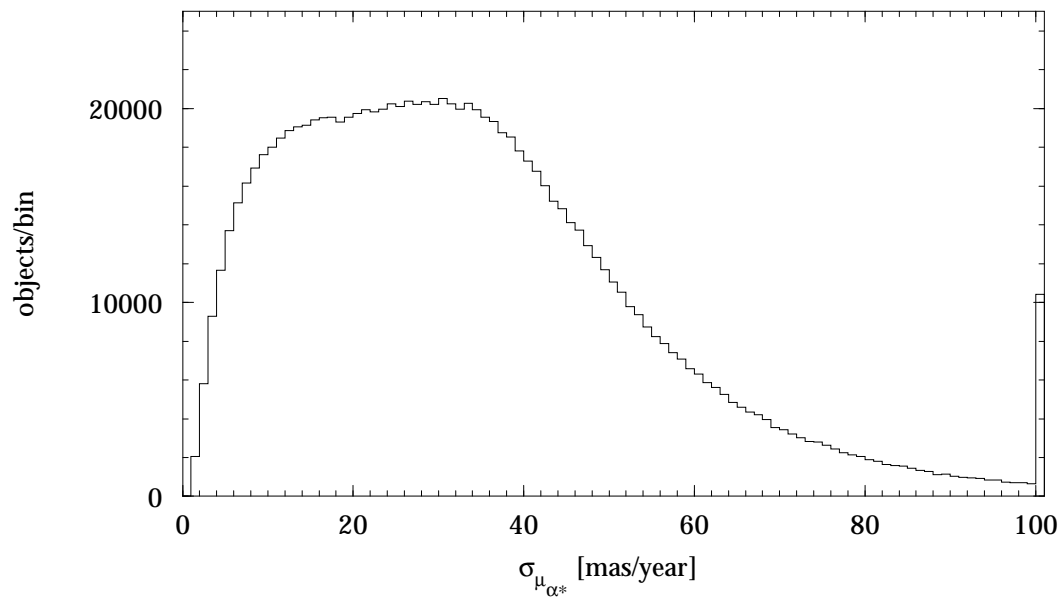


Figure 3.3.18. Tycho Catalogue, Field T17: standard error of μ_{α^*} (bin size 1 mas/year). The rightmost bin contains all values above 100 mas/year.

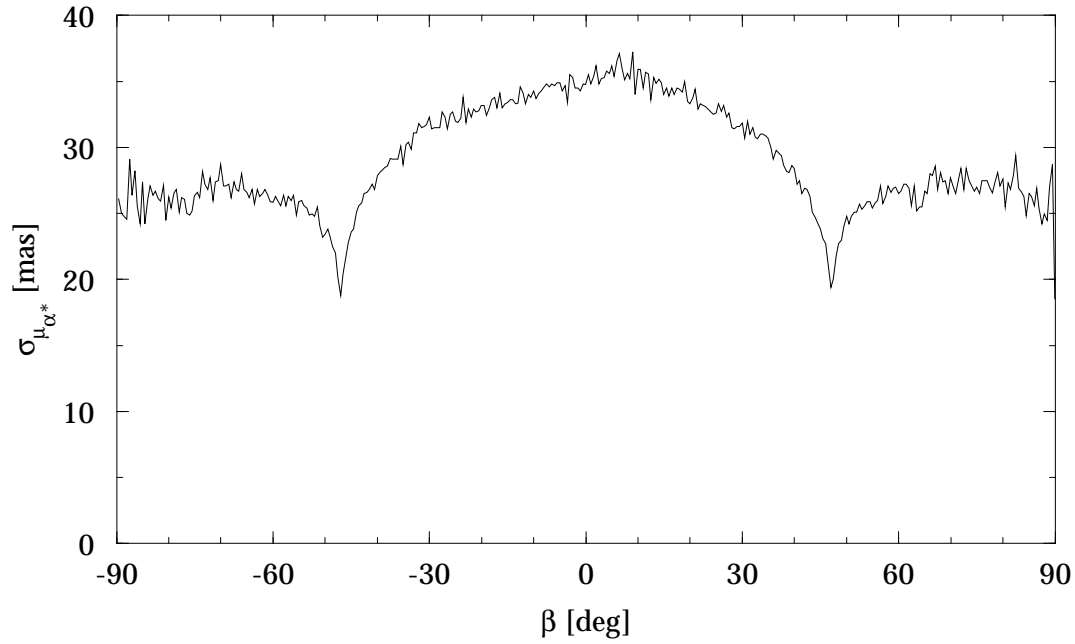


Figure 3.3.19. Tycho Catalogue, Field T17: median standard error of μ_{α^*} versus ecliptic latitude (bin size 0.5°).

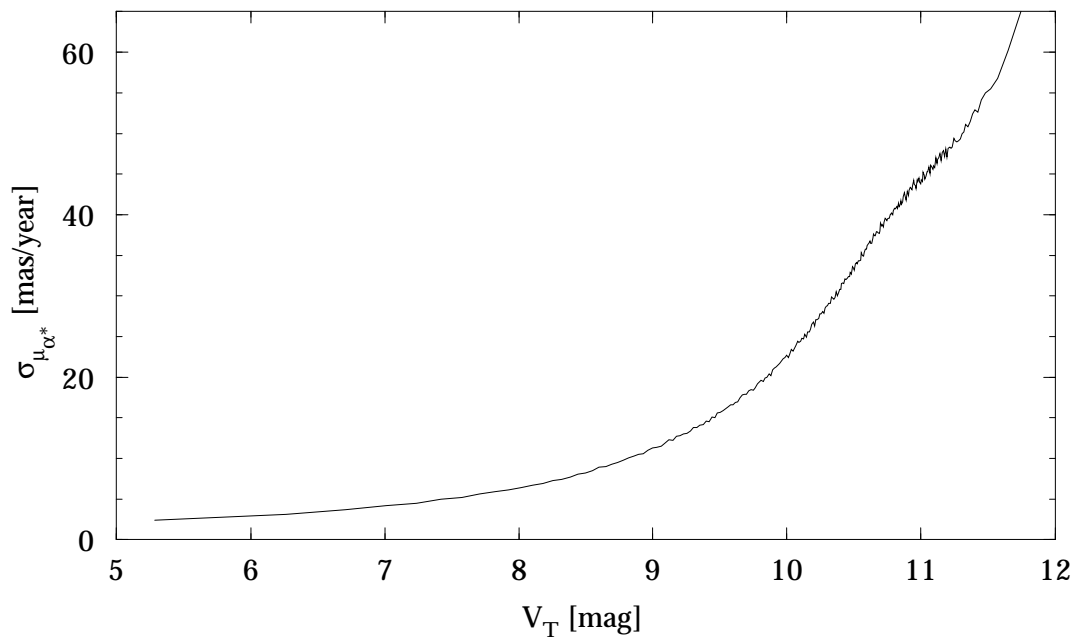


Figure 3.3.20. Tycho Catalogue, Field T17: median standard error of μ_{α^*} versus V_T (bin size 0.05 mag).



Figure 3.3.21. Tycho Catalogue, Field T18: median standard error of μ_δ , in ecliptic coordinates (cell size $3^\circ \times 3^\circ$).

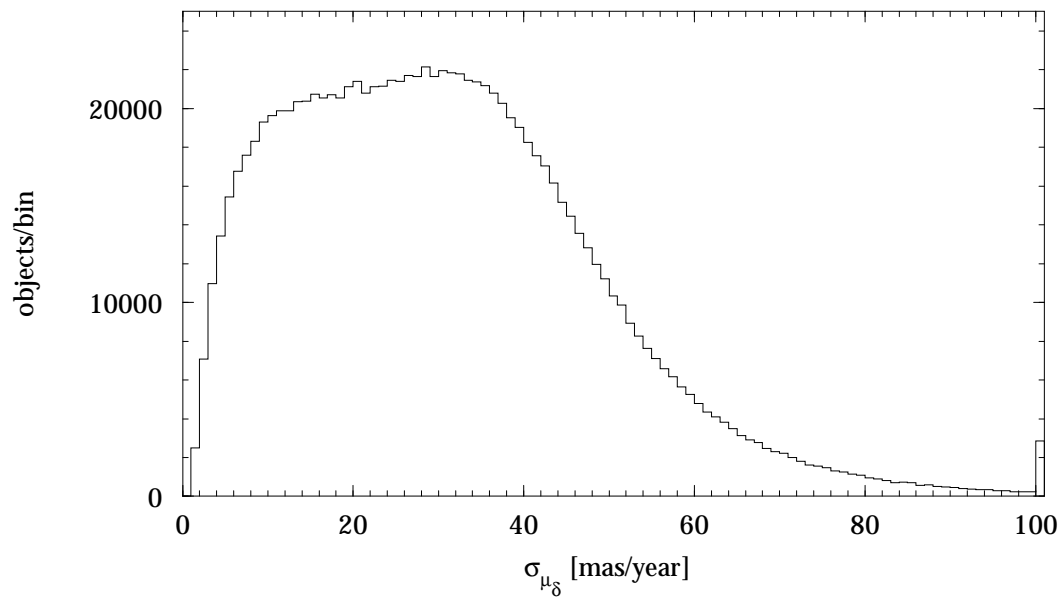


Figure 3.3.22. Tycho Catalogue, Field T18: standard error of μ_δ (bin size 1 mas/year). The rightmost bin contains all values above 100 mas/year.

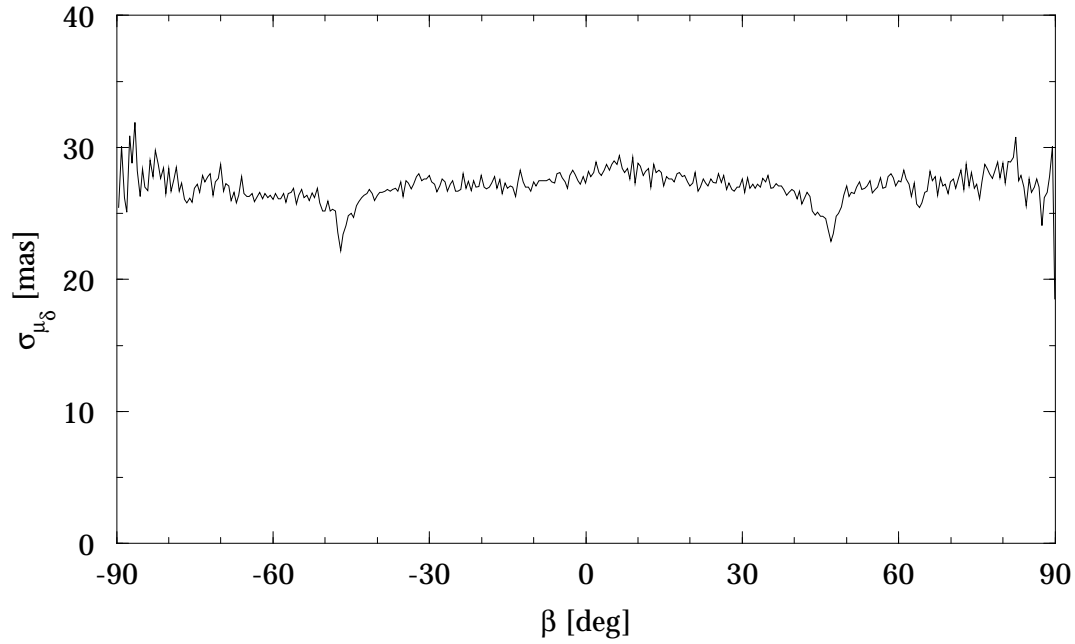


Figure 3.3.23. Tycho Catalogue, Field T18: median standard error of μ_δ versus ecliptic latitude (bin size 0.5°).

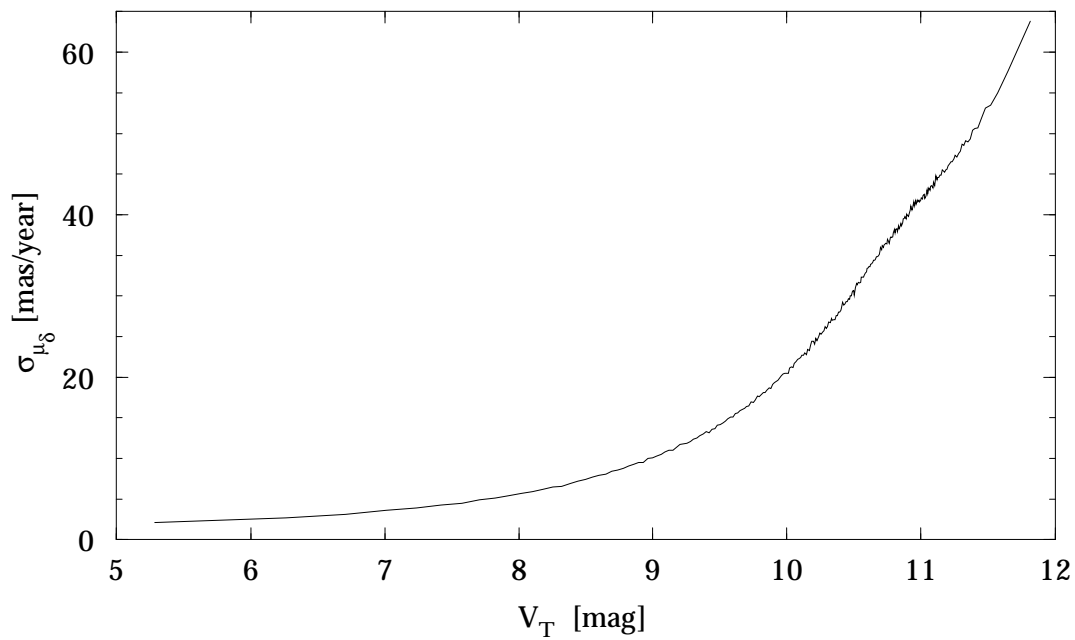


Figure 3.3.24. Tycho Catalogue, Field T18: median standard error of μ_δ versus V_T (bin size 0.05 mag).



Figure 3.3.25. Tycho Catalogue, Field T19: median correlation between α^* and δ in equatorial coordinates (cell size $2^\circ \times 2^\circ$).



Figure 3.3.26. Tycho Catalogue, Field T20: median correlation between α^* and π in equatorial coordinates (cell size $2^\circ \times 2^\circ$).



Figure 3.3.27. Tycho Catalogue, Field T21: median correlation between δ and π in equatorial coordinates (cell size $2^\circ \times 2^\circ$).



Figure 3.3.28. Tycho Catalogue, Field T22: median correlation between α^* and μ_{α^*} in equatorial coordinates (cell size $2^\circ \times 2^\circ$).



Figure 3.3.29. Tycho Catalogue, Field T23: median correlation between δ and μ_{α^*} in equatorial coordinates (cell size $2^\circ \times 2^\circ$).



Figure 3.3.30. Tycho Catalogue, Field T24: median correlation between π and μ_{α^*} in equatorial coordinates (cell size $2^\circ \times 2^\circ$).



Figure 3.3.31. Tycho Catalogue, Field T25: median correlation between α^* and μ_δ in equatorial coordinates (cell size $2^\circ \times 2^\circ$).

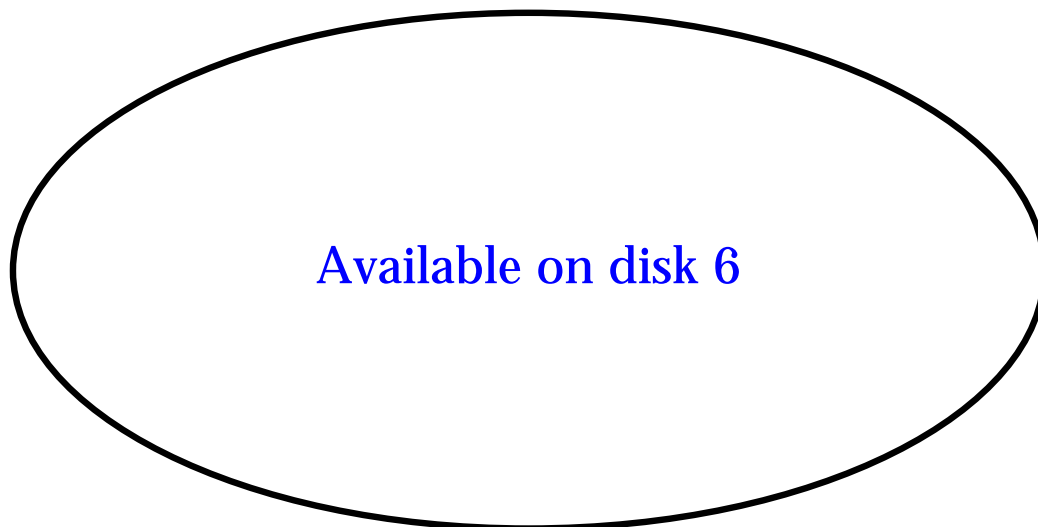


Figure 3.3.32. Tycho Catalogue, Field T26: median correlation between δ and μ_δ in equatorial coordinates (cell size $2^\circ \times 2^\circ$).



Figure 3.3.33. Tycho Catalogue, Field T27: median correlation between π and μ_δ in equatorial coordinates (cell size $2^\circ \times 2^\circ$).



Figure 3.3.34. Tycho Catalogue, Field T28: median correlation between μ_{α^*} and μ_δ in equatorial coordinates (cell size $2^\circ \times 2^\circ$).

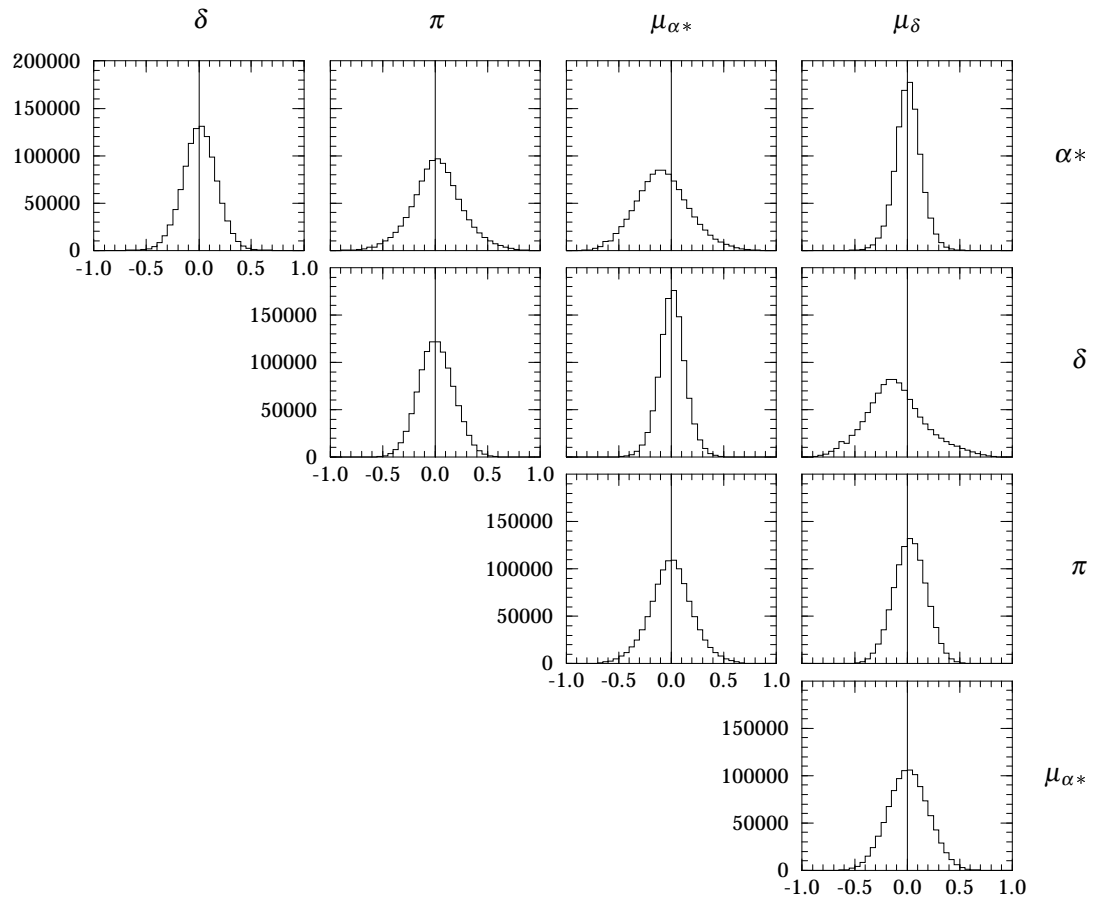


Figure 3.3.35. Tycho Catalogue, Field T19–T28: correlations between astrometric parameters (bin size 0.05).



Figure 3.3.36. Tycho Catalogue, Field T30: median goodness-of-fit parameter, $F2$, in ecliptic coordinates (cell size $3^\circ \times 3^\circ$).

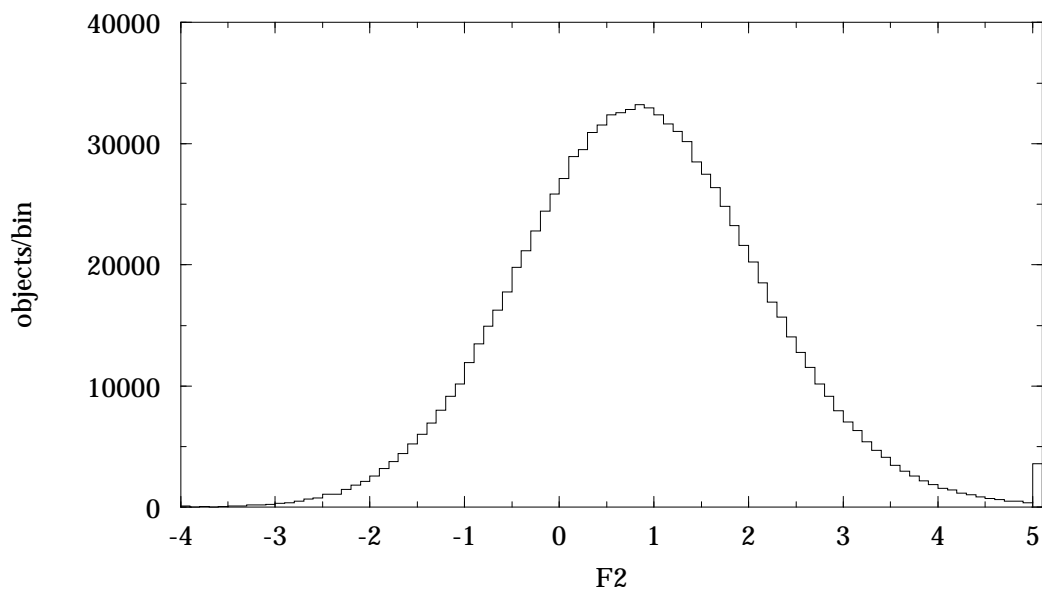


Figure 3.3.37. Tycho Catalogue, Field T30: goodness-of-fit parameter, $F2$ (bin size 0.1). The rightmost bin contains all values above 5.



Figure 3.3.38. Tycho Catalogue, Field T33: median B_T mean magnitude, in equatorial coordinates (cell size $2^\circ \times 2^\circ$).



Figure 3.3.39. Tycho Catalogue, Field T35: median V_T mean magnitude, in equatorial coordinates (cell size $2^\circ \times 2^\circ$).

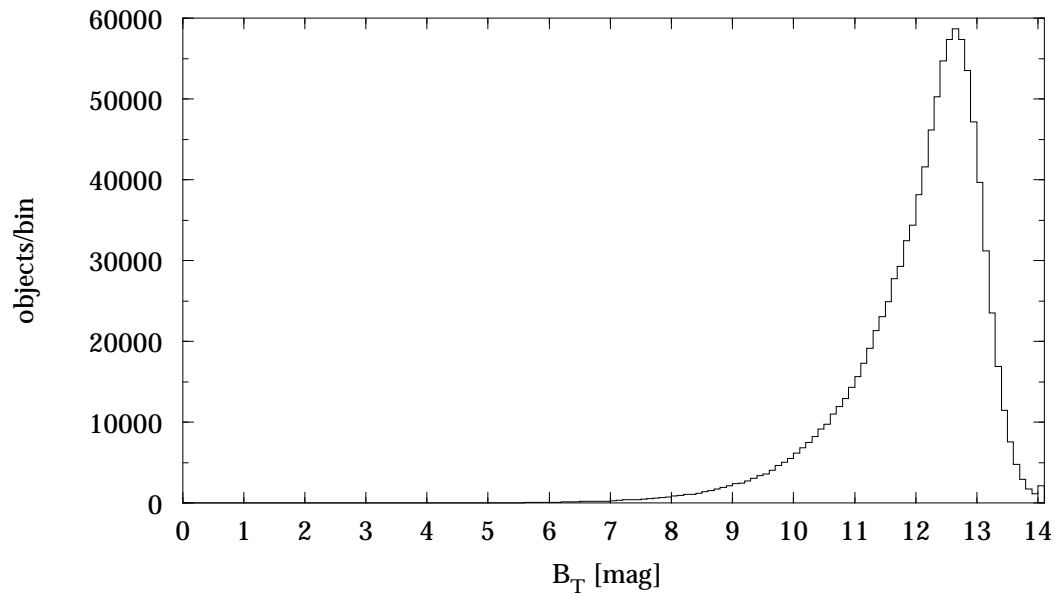


Figure 3.3.40. Tycho Catalogue, Field T33: B_T mean magnitude (bin size 0.1 mag). The rightmost bin contains all values above 14 mag.

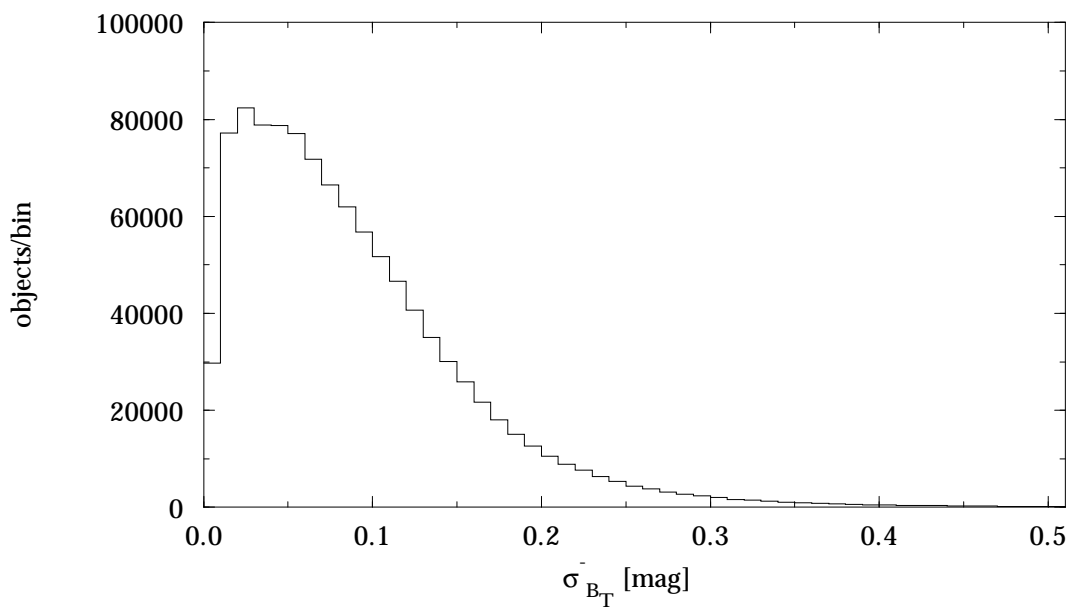


Figure 3.3.41. Tycho Catalogue, Field T34: standard error in B_T mean magnitude (bin size 0.01 mag). The rightmost bin contains all values above 0.5 mag.

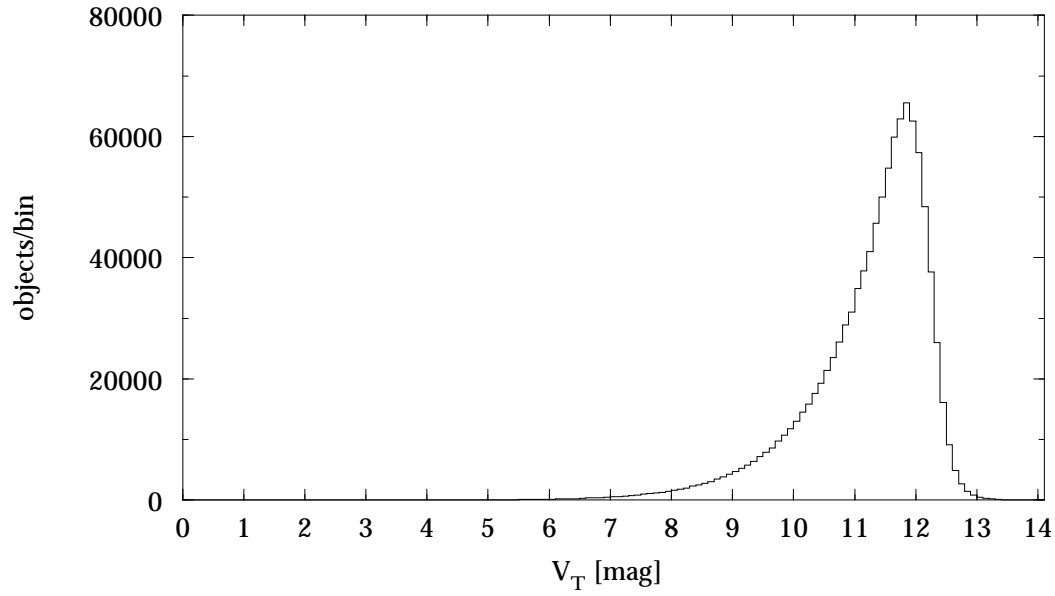


Figure 3.3.42. Tycho Catalogue, Field T35: V_T mean magnitude (bin size 0.1 mag). The rightmost bin contains all values above 14 mag.

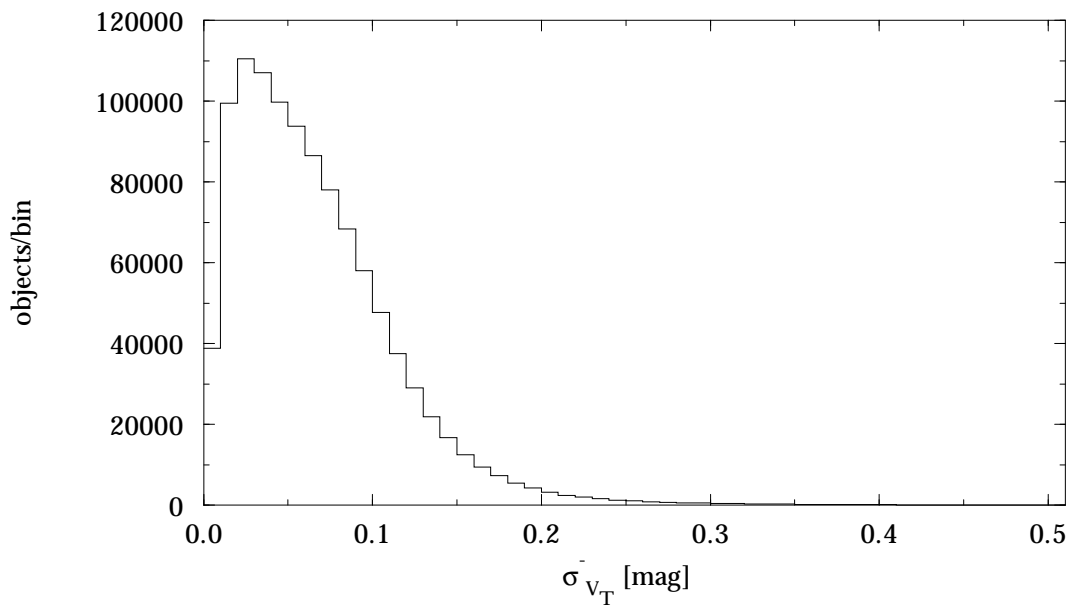


Figure 3.3.43. Tycho Catalogue, Field T36: standard error in V_T mean magnitude (bin size 0.01 mag). The rightmost bin contains all values above 0.5 mag.



Figure 3.3.44. Tycho Catalogue, Field T37: median colour index $B - V$, in galactic coordinates (cell size $3^\circ \times 3^\circ$).

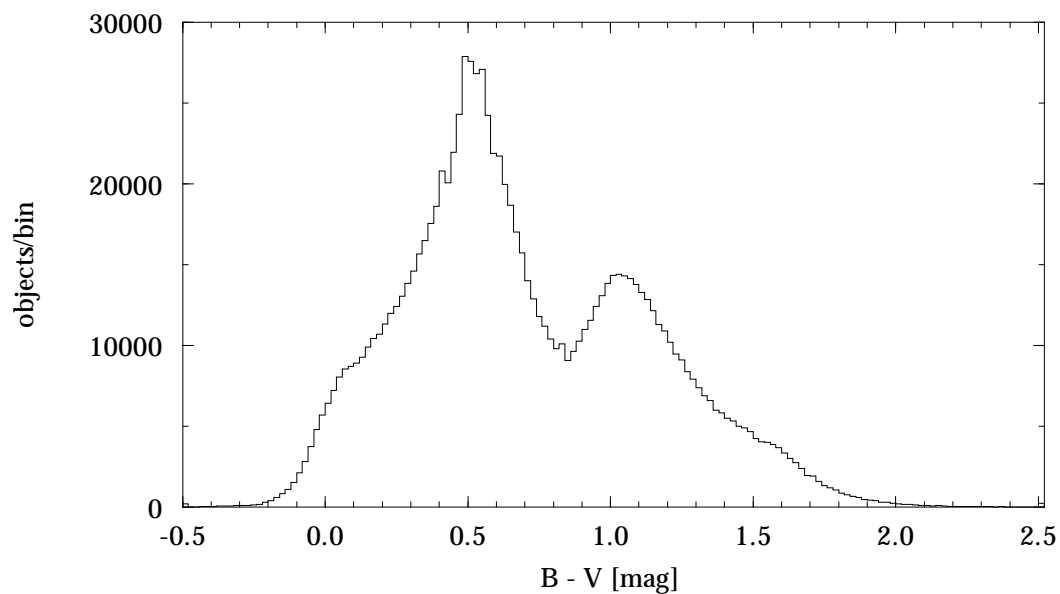


Figure 3.3.45. Tycho Catalogue, Field T37: colour index $B - V$ (bin size 0.02 mag). The rightmost bin contains all values above 2.5 mag.

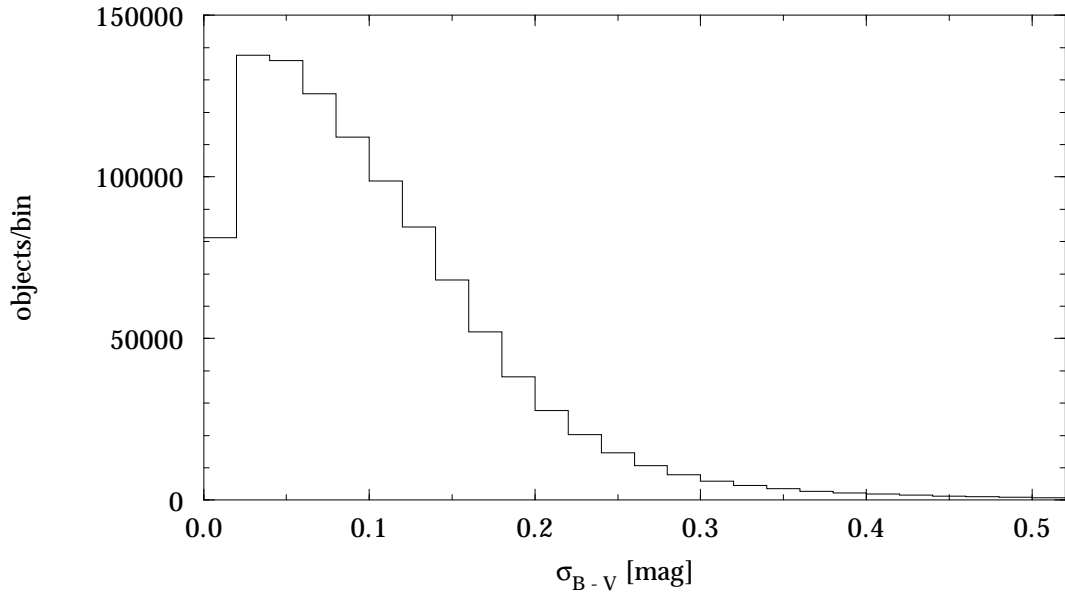


Figure 3.3.46. Tycho Catalogue, Field T38: standard error in colour index $B - V$ (bin size 0.02 mag). The rightmost bin contains all values above 0.5 mag.

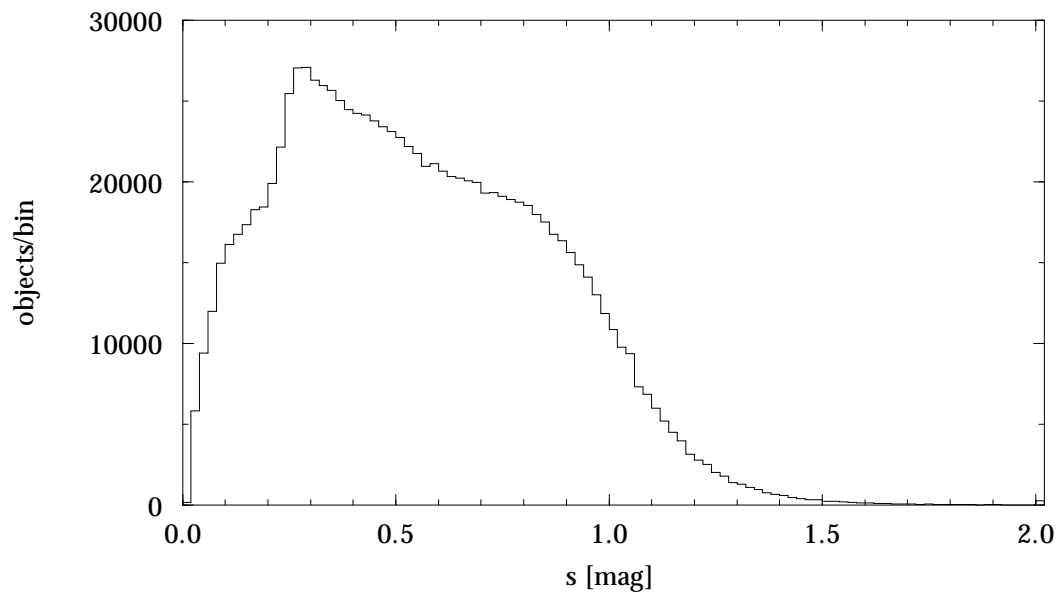


Figure 3.3.47. Tycho Catalogue, Field T44: V_T scatter (bin size 0.02 mag). The rightmost bin contains all values above 2 mag.

